Antlion Optimization for Bending of Arrow Honeycomb

Jiang Hengkun[1], Fang Houfei[2], Hou Yangqing[2], Wu Ke[1]

[1] China Academy of Space Technology (Xi'an), Xi'an 710000, China.
[2] Shanghai YS Information Technology Co., Ltd, Shanghai 200240, China.

* Corresponding author. Tel.: 18729013233; email: hkunjiang@163.com
Manuscript submitted September 5, 2018; accepted March 20, 2019.
doi: 10.17706/ijcce.2020.9.1.54-63

Abstract: In view of the single curved deformation characteristics of zero Poisson's ratio (ZPR) honeycomb, Arrow honeycomb with ZPR is applied to the reflecting surface of the spatial parabolic cylinder antenna in this paper. First of all, the loading method for cylinder formation of honeycomb with ZPR is analysed. Then, Abaqus analysis, surface fitting and precision calculation are integrated into the objective function. Antlion Optimization (ALO) algorithm is used to optimize the RMS error of the deformed surface. The analysis results show that it is feasible to apply the honeycomb with ZPR to the reflector of cylindrical antenna, and the accuracy of deformed profile is improved by 45.5% through the ALO algorithm, which proves the effectiveness and efficiency of the ALO algorithm to solve the problem with unknown initial value. The research results are certainly significant for the optimization design of honeycomb with ZPR and the application of ALO algorithm.

Key words: Zero poisson's ration (ZPR) honeycomb, arrow, cylindrical antenna, antlion optimization (ALO).

1. Introduction

The structure of parabolic cylinder antenna has been preliminarily studied in the late 20th century and further developed in the early 21st century. In 2003, John k. Lin *et al*. [1] demonstrated the feasibility of technology which meet the precision requirements through the development of the membrane structure and the precision test of the molded surface. In 2004, British O.Soykasap *et al*. [2] conducted the research of the bidirectional deployable elastic shell parabolic cylinder antenna. In 2004, Christopher g. Meyer *et al*. [3] discovered the influence of boundary support conditions and gravity acceleration on the reflector of a thin film parabolic cylinder in orbit. In 2007, Eastwood Im *et al*. [4] designed a half-size prototype PR-2 parabolic cylinder antenna. In 2010, Jack Leifer *et al*. [5] studied the shape variation of parabolic films under different gravity conditions.

At the early stage of the research, antenna reflector is made of metal materials which are heavy and stiff, and the membrane is easy to fold to influence the precision. All of these limit the development of diameter and the scope of applications [6], [7].Compared with other traditional materials, honeycomb is characterized by light weight, high strength, stiffness and shear modulus, shock resistance, heat insulation, designability and stress concentration reduction. The deformation of the structure with ZPR will not produce coupling in the orthogonal direction. Similarly, when the structure with ZPR is bending, it usually appears as cylinder [8].Honeycombs such as Silicomb [9], [10], Chevron [11] and Accordion [12] which usually have a Poisson's ratio of zero. ZPR structures under external bending deform like a single curve, as shown in Fig. 1, which makes the structure more suitable for the single curvature bending deformation [8],

[13].

In this paper, Arrow honeycomb will be applied to fit parabolic antenna reflector to demonstrate the feasibility of the ZPR honeycombs used for parabolic antenna and the effectiveness of ALO algorithm, and accuracy will be optimized through ALO algorithm.

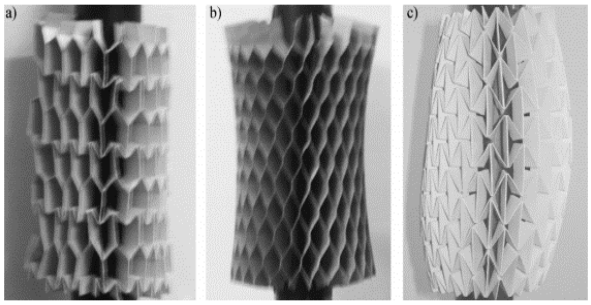

Fig. 1. Images of ‘‘tubes’’ formed from honeycombs with: (a) ZPR-single curve (b) PPR-concave (c) NPR-convex.

2. Cylinder Formation

In this paper, the ZPR honeycomb Arrow is selected as the research object and the ideal surface is parabolic cylinder. The model (122*100*2.5(mm)) of honeycomb panel is established by UG-NX, as shown in Fig. 2. ABAQUS is adopted in the analysis and calculation, and the element is S4R.

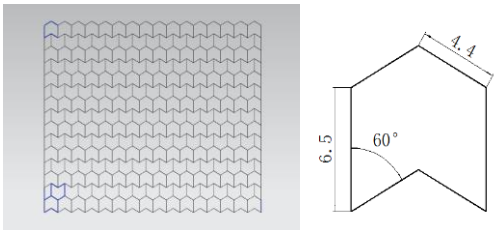

Fig. 2. Geometry of Arrow honeycomb.

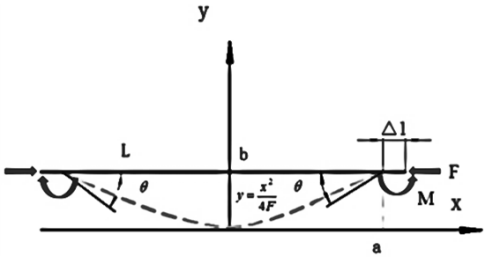

Fig. 3. Illustration of loading method.

Assuming that the length of the honeycomb panel will not change before and after deformation, symmetric rotation and displacement loads are applied to both sides of the panel, as shown in Fig. 3. The parameters in the figure are expressed as follows:

$$L = \int_{-a}^{a} \sqrt{1 + y'^2}\, d \tag{1}$$

$$\Delta l = \frac{L}{2} - a \tag{2}$$

$$tan\theta = y'(a) \tag{3}$$

where L is the original length of honeycomb panel, y is the target curve.

In fact, the influence of thickness cannot be ignored due to the dimension limitation of the panel. So the (2) should be amended as follows:

$$\Delta l = \frac{L}{2} - a + \frac{h}{2} \times cos\theta \tag{4}$$

where h is the thickness of panel.

FE analysis is carried out according to the calculated loads. The plot contour shows the consistency of the deformation along width direction, as shown in Fig. 4. The bending deflection proves the effectiveness of the parabolic cylinder and the feasibility of ignoring the influence of width. The value of required loads is obtained through geometric calculations above. Although the influence of thickness of the panel has been considered, the precision of the cylinder isn't the highest because of the nonlinear deformation during bending process. So the value of loads need to be further optimized.

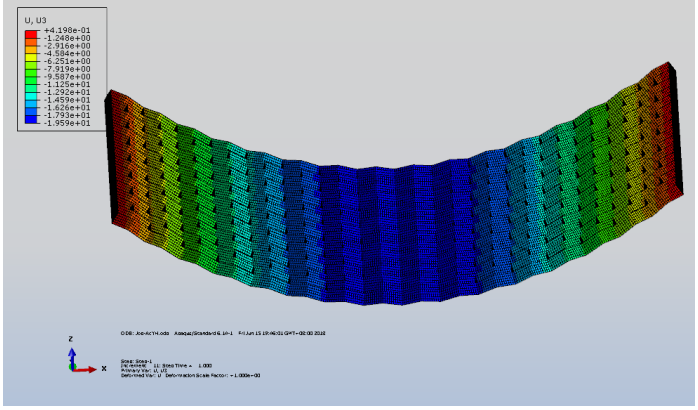

Fig. 4. FE simulation of honeycomb deformation.

3. Overview of Antlion Optimization algorithm

The Antlion Optimization algorithm is a novel optimization algorithm which mimics the hunting process of antlions in nature. It was first proposed by Australian scholar Mirjalili in 2015 [14]. An antlion larvae digs a cone-shaped pit by rotating in the sand as it drills down [15]-[17]. It hides under the bottom of the funnel and waits for insects to be trapped [18]. When ants or other insects climb into traps, they slide down because of loose sands, antlion will cast sands out continuously. Then antlions with large jaws will clamp their prey and eat it under the sand. Then the corpse will be thrown out of the trap for the next hunting [19].

3.1. Operators of the ALO Algorithm

The ALO algorithm mimics the interaction between antlion and ant in the process of predation, as shown in Fig. 5. Ants are required to move in the search space, while antlions capture them and become more adaptable by building traps for prey. To model the interaction process, a random walk of ants is simulated as follows:

$$X(t) = [0, cumsum(2r(t_1) - 1), cumsum(2r(t_{12}) - 1), \cdots, cumsum(2r(t_n) - 1)] \tag{5}$$

where n is the maximum number of iterations, t is the step of random walk, *cumsum* calculates the cumulative sum, and *r(t)* is expressed as follows:

$$r(t) = \begin{cases} 1 \; if \; rand > 0.5 \\ 0 \; if \; rand \leq 0.5 \end{cases} \tag{6}$$

In the optimization process, the location of ants are stored in following matrix:

$$M_{Ant} = \begin{matrix} Ant_{1,1} & Ant_{1,2} & \cdots & Ant_{1,d} \\ Ant_{2,1} & Ant_{2,2} & \cdots & Ant_{2,d} \\ \vdots & \vdots & \ddots & \vdots \\ Ant_{n,1} & Ant_{n,2} & \cdots & Ant_{n,d} \end{matrix} \tag{7}$$

where *Anti,j* is the *j-th* value of the *i-th* ant, *n* is the number of ants, and *d* is the number of variables. Each ant's location represents an optimal parameter value. The fitness matrix of ants is calculated by using the objective function:

$$M_{OA} = \begin{bmatrix} F([Ant_{1,1}, Ant_{1,2}, \cdots, Ant_{1,d}]) \\ F([Ant_{2,1}, Ant_{2,2}, \cdots, Ant_{2,d}]) \\ \vdots \\ F([Ant_{n,1}, Ant_{n,2}, \cdots, Ant_{n,d}]) \end{bmatrix} \tag{8}$$

where *F* is the objective function. Similarly, the antlions are hiding in the search space, the location matrix and fitness matrix can also be expressed as follows:

$$M_{AntL} = \begin{matrix} AntL_{1,1} & AntL_{1,2} & \cdots & AntL_{1,d} \\ AntL_{2,1} & AntL_{2,2} & \cdots & AntL_{2,d} \\ \vdots & \vdots & \ddots & \vdots \\ AntL_{n,1} & AntL_{n,2} & \cdots & AntL_{n,d} \end{matrix} M_{OAL} = \begin{bmatrix} F([AntL_{1,1}, AntL_{1,2}, \cdots, AntL_{1,d}]) \\ F([AntL_{2,1}, AntL_{2,2}, \cdots, AntL_{2,d}]) \\ \vdots \\ F([AntL_{n,1}, AntL_{n,2}, \cdots, AntL_{n,d}]) \end{bmatrix} \tag{9}$$

where *AntLi,j* is the *j-th* value of the *i-th* antlion, *n* is the number of antlions, *d* is the number of variables, and *F* is the objective function.

3.1.1. Random walks of ants

Ants change their location randomly through (5). In order to ensure the ants walk inside the search space, they need to be normalized using following equation:

$$X_i^t = \frac{(X_i^t - a_i) \times (d_i^t - c_i^t)}{(b_i - a_i)} + c_i^t \tag{10}$$

where a_i is the minimum of random walk of *i-th* variable, b_i is the maximum of random walk of *i-th* variable, c_i^t is the minimum of random walk of *i-th* variable at *t-th* iteration, d_i^t is the maximum of random walk of *i-th* variable at *t-th* iteration.

3.1.2. Trapping in pits

Random walks of ants are affected by traps of antlions. This behavior can be described as follows:

$$c_i^t = Antlion_j^t + c^t \tag{11}$$

$$d_i^t = Antlion_j^t + d^t \tag{12}$$

where c^t is the minimum of all variables at *t-th* iteration; d^t is the maximum of all variables at *t-th* iteration; c_i^t is the minimum of all variables for *i-th* ant; d_i^t is the maximum of all variables for *i-th* ant; $Antlion_j^t$ is the position of *j-th* antlion at *t-th* iteration.

3.1.3. Building trap

Antlion optimization algorithm mimics the behavior of the antlion predation in nature by a roulette wheel. Antlion is selected based on their fitness to optimization progress. The mechanism gives more chances to the fitter antlions for catching ants.

3.1.4. Sliding ants towards antlions

Once the antlion realizes that an ant is in the trap, it will throw sands out of the center of the trap to make

the ant trying to escape slide down slowly. The following equations are presented in this regard:

$$c^t = \frac{c^t}{I} \tag{13}$$

$$d^t = \frac{d^t}{I} \tag{14}$$

where I is the ratio. In (13) and (14), $I = 10^W \times \frac{t}{T}$. Where t is the current iteration, T is the maximum number of iteration, and W is a constant based on the current iteration as follows:

$$W = \begin{cases} 2 & t > 0.1T \\ 3 & t > 0.5T \\ 4 & t > 0.75T \\ 5 & t > 0.9T \\ 6 & t > 0.95T \end{cases}$$

Basically, the constant W adjust the accuracy level of optimization algorithm.

3.1.5. Catching prey and re-building the trap

If the ant has a better fitness than the selected antlion then it changes its position to the largest position of the hunted ant to improve its chance of catching new one. The following equation is illustrated in this regard:

$$Antlion_j^t = Ant_i^t \; if \; F(Ant_i^t) > F(Antlion_j^t) \tag{15}$$

where t shows the current iteration, $Antlion_j^t$ shows the position of j-th antlion at t-th iteration, Ant_i^t indicates the position of i-th ant at t-th iteration.

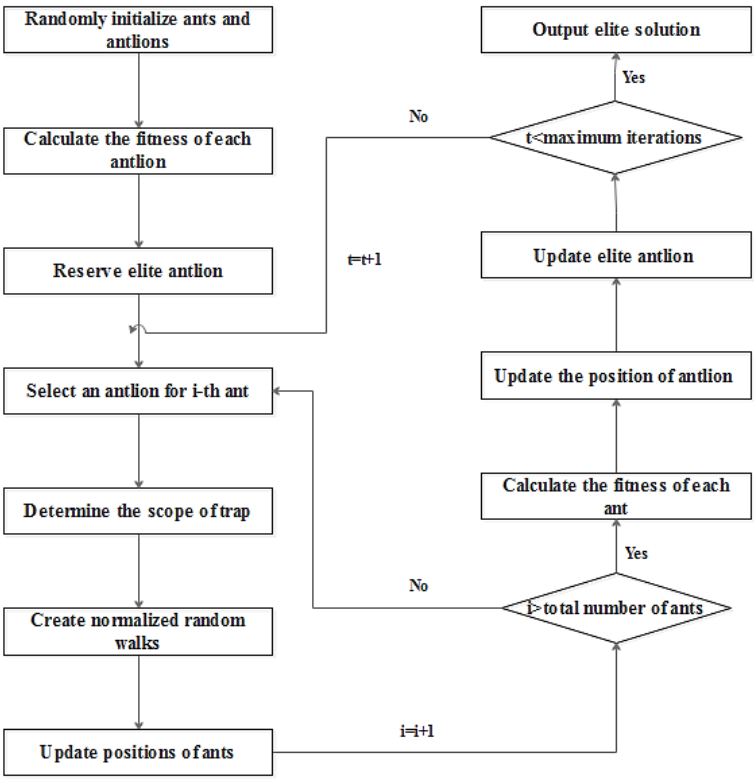

Fig. 5. Flow chart of ALO.

3.1.6.Elitism

In this algorithm, the best antlion obtained so far in each iteration is saved as an elite. Since the elite is the fittest antlion, it can affect all the ants during the iterations. Thus, it is assumed that every ant randomly walks around a chosen antlion by the roulette wheel and the elite simultaneously as follows:

$$Ant_i^t = \frac{R_A^t + R_E^t}{2} \tag{16}$$

where R_A^t is the random walk around the antlion selected by roulette wheel at *t-th* iteration, R_E^t is the random walk around the elite at *t-th* iteration.

4. Results

RMS error represents the difference between the deformed surface by different loads and the ideal one. It can be given by:

$$\text{rms} = \sqrt[2]{\sum_i^n ((\Delta x)^2 + (\Delta y)^2)/n} \tag{17}$$

All the nodes on the surface of the inner deformed honeycomb are taken into account. And the optimal fitting of the node set is required before RMS error calculation [20], [21].

As mentioned in section 1, the loads are obtained by geometric calculation. When the thickness of the panel is not taken into account ((2) and (3)), the results are:

$$\theta = 0.616\text{rad}, \Delta l = 4.4\text{mm}.$$

Whereas, if the thickness of the honeycomb panel is taken into account, the results derived from (4) are:

$$\theta = 0.616 \text{ rad}, \Delta l = 5.12 \text{ mm}.$$

The loads are respectively applied to the honeycomb panel in ABAQUS, and then the RMS error of the deformed surface is calculated. The results are shown in Fig. 6.

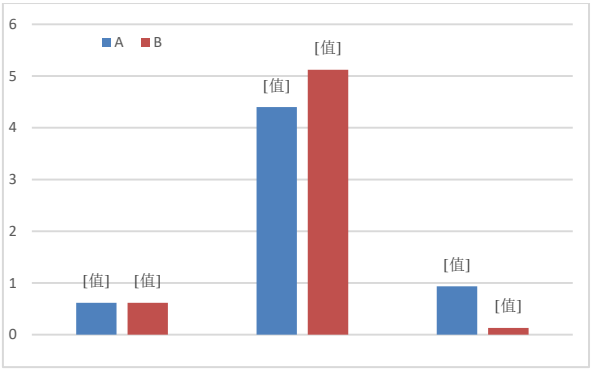

Fig. 6. Result of geometric loads.

In the figure, series B represents that the thickness of the panel is considered, while series A represents the opposite situation. It can be seen that in the geometric calculation, the thickness only influences the displacement. When the loads derived from (4) are applied, the precision of the surface is greatly improved, and the RMS error is reduced by 86.0% in comparison. That means when the thickness of the panel is not negligible compared with its dimension, the thickness must be considered in the loads calculation.

In this paper, the Antlion Optimization algorithm (ALO) is applied to optimize the precision of the

deformed surface, then to validate the effectiveness and excellent performance of ALO. The algorithm iteration process is shown in Fig. 7.

The results show that the Arrow honeycomb with ZPR can form a parabolic cylinder with a certain precision. Meanwhile, when ALO algorithm is used to solve the optimization problem, the iteration tends to be converged quickly. The results are shown as follows:

θ=0.5883 rad; Δl=5.0530 mm; RMS=0.0713mm.

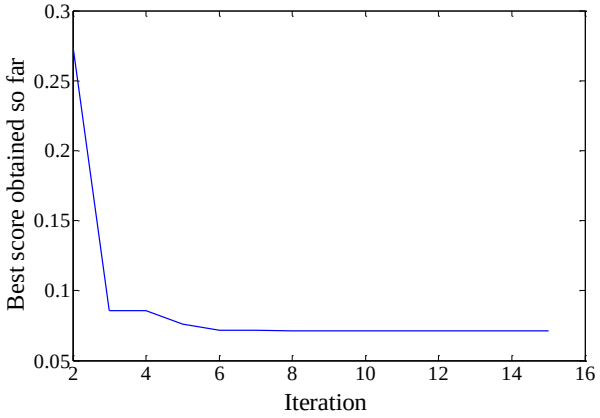

Fig. 7. Convergence curve of ALO algorithm.

The results show that ALO algorithm is effective. Compared with geometric deformation results, RMS error decreases by about 45.5%.The ALO algorithm can solve the optimization problem efficiently and quickly. The variation trend of its target value will not fluctuate greatly during the iteration, which also proves the high computational efficiency of ALO.

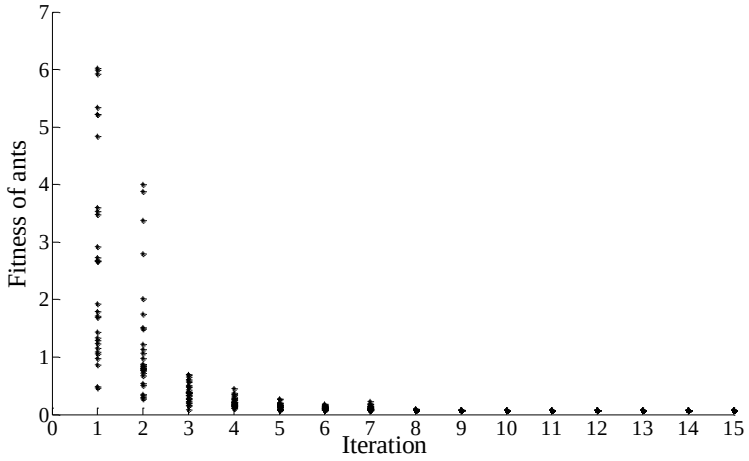

Fig. 8. Search history of ALO algorithm.

Fig. 8 shows the fitness of each ant during the iteration. It can be seen that as the iteration proceeding, all ants are gradually approaching, which indicates that the random walk of all ants is decreasing. This figure proves the convergence of ALO algorithm. The position of the ant with the highest fitness in each iteration will accordingly update the position of the elite.

Compared with ALO algorithm, Active Set algorithm begins to converge after 35th iteration, which means its convergence speed is slower than ALO algorithm about seven times. And it can be seen at Fig. 9 that the objective function values in the process of convergence has a lot of volatility, while ALO algorithm converges

smoothly and quickly during iteration, which proves its high efficiency of convergence property of ALO algorithm. Also, because the output of ALO algorithm is almost the same as it of Active Set algorithm, the validity of ALO algorithm is demonstrated.

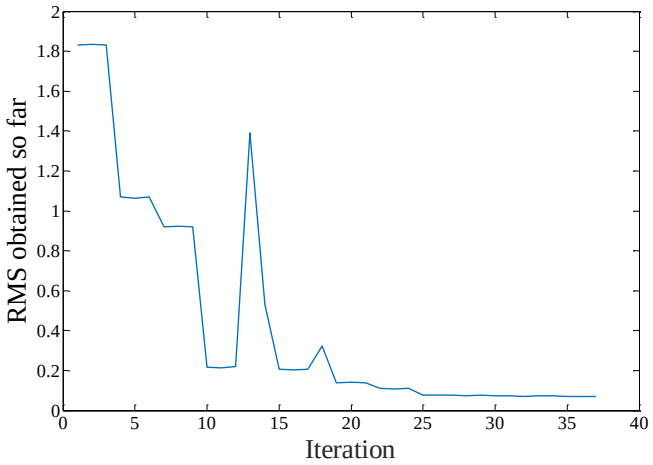

Fig. 9. Convergence curve of active set algorithm.

In addition, it is important to note that in the process of Active Set algorithm, the results will be directly affected by variable selection of initial value. If the difference between initial value and target value is great, it will cause local convergence problems easily. Thus, the reason why Active Set algorithm receives the same result as ALO algorithm is using geometric loads as the initial values. Whereas, ALO algorithm does not need an initial value for the variable.

5. Conclusion

In this paper, the Arrow honeycomb with ZPR is applied to form a parabolic cylinder by means of the combination of rotation and displacement. The RMS error is further reduced by using the ALO algorithm, which further improves the precision of the shaped surface of the parabolic cylinder. The optimization results fully prove the feasibility of applying the Arrow honeycomb to the parabolic cylinder antenna to make a high-precision reflector. Meanwhile, the ALO algorithm adopted in the optimization process also shows excellent performance, which can avoid the local optimal result very well. The algorithm itself and the target problem are independent from each other, and are not related to the initial value, which proves the feasibility of ALO algorithm for solving various optimization problems in reality.

Conflict of Interest

The authors declare no conflict of interest.

Author Contributions

All authors had approved the final version.

References

[1] John, K. L., George, H. S., Stephen, E. S., *et al*. (2003). Advanced precipitation radar antenna singly curved parabolic antenna reflector development. *Proceedings of the 44th AIAA/ ASME/ASCE/AHS Structures, Structural Dynamics, and Materials Conference* (pp. 7-10). Norfolk.

[2] Sovkasap, O, Watt, A. M., & Pellegrino, S. (2004). New deployable reflector concept. *Proceedings of the 45th AIAA/ASME/ ASCE/AHS/ASC Structures, Structural Dynamics & Materials Conference* (pp. 19-22).

Palm Springs.

[3] Greschik, G., Mikulas, M. M., & Palisoc, A. (2004). Torus-less inflated membrane reflector with an exact parabolic center. *AIAA Journal*, *42(12)*, 2579-2584.

[4] Im, E., & Durden, S. L. (2007). Next-generation spaceborne precipitation radar instrument concepts and technologies. *Proceedings of the 45th AIAA Aerospace Sciences Meeting and Exhibit* (pp. 8-11). Reno.

[5] Leifer, J., Jones, D. C., & Cook, A. M. (2012). Gravity-induced wrinkling in subscale, singly curved parabolic gossamer membrane. *Journal of Spacecraft & Rockets*, *47(1)*, 214-219.

[6] Yuan, S., Yang, B., & Fang, H. (2018). Form-finding of large deployable mesh reflectors with elastic deformations of supporting structures. *Proceedings of the AIAA Spacecraft Structures Conference, AIAA SciTech Forum* (p. 1198).

[7] Shi, H., Yuan, S., & Yang, B. (2018). New methodology of surface mesh geometry design for deployable mesh reflectors. *Journal of Spacecraft and Rockets*, *55(2)*, 266-281.

[8] Grima, J. N., Oliveri, L., Attard, D., *et al*. (2010). Hexagonal honeycombs with zero Poisson's ratios and enhanced stiffness . *Advanced Engineering Materials, 12(9)*, 855-862.

[9] Neville, R. M., Monti, A., Hazra, K., *et al*. (2014). Transverse stiffness and strength of Kirigami zero-ν PEEK honeycombs. *Composite Structures*, *114(1)*, 30-40.

[10] Scarpa, F., Chen, Y., Remillat, C., *et al*. (2014). Curved Kirigami SILICOMB cellular structures with zero Poisson's ratio for large deformations and morphing. *Journal of Intelligent Material Systems & Structures*, *25(6)*, 731-743.

[11] Grima, J. N., Oliveri, L., Attard, D., *et al*. (2010). Hexagonal honeycombs with zero Poisson's ratios and enhanced stiffness. *Advanced Engineering Materials*, *12(9)*, 855-862.

[12] Painter, R., Remillat, C. D. L., Scarpa, F., *et al*. (2014). A morphing mechanical and electromagnetic antenna reflector concept based on curved corrugated structures. *Proceedings of the ICAST 25th International Conference on Adaptive Structures and Technologies*. Hague.

[13] Olympio, K. R., & Gandhi, F. (2010). Zero Poisson's ratio cellular honeycombs for flex skins undergoing one-dimensional morphing. *Journal of Intelligent Materials Systems & Structure*, *21(21)*, 1737-1753.

[14] Mirjalili, S. (2015). The ant lion optimizer. *Advanced in Engineering Software, 83(C)*, 80-98.

[15] Nischal, M. M., & Mehta, S. (2015). Optimal load dispatch using ant lion optimization. *Journal of Engineering Research and Applications, 5(8),* 10-19.

[16] Scharf, I., Subach, A., & Ovadia, O. (2008). Foraging behaviour and habitat selection in pit building antlion larvae in constant light or dark conditions. *Animal Behaviour, 76(6),* 2049-2057.

[17] Griffiths, D. (1986). Pit construction by ant-lion larvae: A cost-benefit analysis. *Journal of Animal Ecology, 55(1),* 39-57.

[18] Goodenough, J., Mcguire, B., & Jakob, E. (1993). Perspectives on animal behavior. *Wiley & Sons, 45(95)*.

[19] Scharf, I., & Ovadia, O. (2006). Factors influencing site abandonment and site selection in a sit-and-wait predator: A review of pit-Building antlion larvae. *Journal of Insect Behavior, 19(2),* 197-218.

[20] Yuan, S., Yang, B., & Fang, H. (2016). Improvement of surface accuracy for large deployable mesh reflectors. *Proceedings of the AIAA/AAS Astrodynamics Specialist Conference, AIAA SPACE Forum* (p. 5571).

[21] Yuan, S., & Yang, B. (2016). Design and optimization of tension distribution for space deployable mesh reflectors. *Proceedings of the 26th AAS/AIAA Space Flight Mechanics Meeting* (pp. 765-776).

Jiang Hengkun was born in October, 1994 in China. He received his bachelor in Northwestern Polytechnical University, Xi'an, China (2012-2016) with major of mechanical design, manufacture and automation. He got the master in China Academy of Space Technology (Xi'an), Xi'an, China (2016-) with major of aerospace science and technology. His research interests are structure design technology of spacecraft antenna and electronic equipment.